Invited Article: High-pressure techniques for condensed matter physics at low temperature

Yejun Feng, R. Jaramillo, Jiyang Wang, Yang Ren, and T. F. Rosenbaum

Citation: Review of Scientific Instruments **81**, 041301 (2010); doi: 10.1063/1.3400212
View online: http://dx.doi.org/10.1063/1.3400212
View Table of Contents: http://scitation.aip.org/content/aip/journal/rsi/81/4?ver=pdfcov
Published by the AIP Publishing

Invited Article: High-pressure techniques for condensed matter physics at low temperature

Yejun Feng,[1,2] R. Jaramillo,[3] Jiyang Wang,[2] Yang Ren,[1] and T. F. Rosenbaum[2]
[1]*The Advanced Photon Source, Argonne National Laboratory, Argonne, Illinois 60439, USA*
[2]*The James Franck Institute and Department of Physics, The University of Chicago, Chicago, Illinois 60637, USA*
[3]*School of Engineering and Applied Science, Harvard University, Cambridge, Massachusetts 02138, USA*

(Received 12 October 2009; accepted 27 March 2010; published online 20 April 2010)

Condensed matter experiments at high pressure accentuate the need for accurate pressure scales over a broad range of temperatures, as well as placing a premium on a homogeneous pressure environment. However, challenges remain in diamond anvil cell technology, including both the quality of various pressure transmitting media and the accuracy of secondary pressure scales at low temperature. We directly calibrate the ruby fluorescence $R1$ line shift with pressure at T=4.5 K using high-resolution x-ray powder diffraction measurements of the silver lattice constant and its known equation of state up to P=16 GPa. Our results reveal a ruby pressure scale at low temperatures that differs by 6% from the best available ruby scale at room T. We also use ruby fluorescence to characterize the pressure inhomogeneity and anisotropy in two representative and commonly used pressure media, helium and methanol:ethanol 4:1, under the same preparation conditions for pressures up to 20 GPa at T=5 K. Contrary to the accepted wisdom, both media show equal levels of pressure inhomogeneity measured over the same area, with a consistent $\Delta P/P$ per unit area of $\pm 1.8\ \%/(10^4\ \mu\mathrm{m}^2)$ from 0 to 20 GPa. The helium medium shows an essentially constant deviatoric stress of 0.021 ± 0.011 GPa up to 16 GPa, while the methanol:ethanol mixture shows a similar level of anisotropy up to 10 GPa, above which the anisotropy increases. The quality of both pressure media is further examined under the more stringent requirements of single crystal x-ray diffraction at cryogenic temperature. For such experiments we conclude that the ratio of sample-to-pressure chamber volume is a critical parameter in maintaining sample quality at high pressure, and may affect the choice of pressure medium. © *2010 American Institute of Physics.*
[doi:10.1063/1.3400212]

I. INTRODUCTION

Diamond anvil cell techniques provide gigapascal pressures in the laboratory with great consequence for condensed matter physics, where the energy density of the applied pressure is well matched to the characteristic electronic and magnetic energy scales in a broad spectrum of materials of interest. However, compared to the typical pressure conditions used in geophysical research for which the diamond anvil cell was originally developed, condensed matter physics research at high pressure presents a new set of technical constraints. The absolute scale of pressure must be known to great accuracy in the vicinity of phase changes and over a range of temperatures, including the limit of zero temperature for quantum phase transitions. Moreover, as compared to magnetic fields or uniaxial stress, hydrostatic pressure can serve as a tuning parameter without introducing a symmetry-breaking field, but only as long as pressure gradients are kept to a minimum. We describe here experiments that quantify the homogeneity of standard pressure media used in diamond anvil cell investigations as well as the essential response of common manometers, with an emphasis on low temperatures where both nonhydrostatic conditions[1–4] and a lack of accuracy in existing pressure scales[5,6] continue to hamper researchers.

Every high-pressure experiment begins with the choice of a pressure medium. Historically, solid pressure media such as NaCl, AgCl, and talc/steatite were widely used in opposed-anvil high-pressure cells. Silicone oil and Fluorinert remain common choices in clamp cells up to 2 GPa. Contemporary choices of pressure media for diamond anvil cells fall into two categories: either (1) condensed gases such as helium, neon, nitrogen, or argon, or (2) mixtures of organic fluids like methanol:ethanol 4:1 and iso-n-pentanes 1:1. Helium and methanol:ethanol 4:1 are the two most widely used pressure media, as they are the best representative of each class and remain liquid at room temperature up to 12.1 and 10.5 GPa, respectively.[1,4] However, both are solids for P>0.02 GPa at T=5 K, and there has been very limited study of their characteristics, such as pressure inhomogeneity and anisotropy, at cryogenic temperatures. Given the growing interest in condensed matter physics at high pressure, a quantitative study of these issues is desirable.

Another unresolved issue is that of pressure calibration at low temperature. Most modern high-pressure techniques such as the diamond anvil cell are incompatible with primary pressure calibration. Of the secondary techniques available, those that depend on known equations of state (EOSs) are perhaps the most dependable. Measuring static pressures in

the range of 1–100 GPa is, *in principle*, a test of our understanding of the EOS for certain simple-structured materials, such as Cu, Ag, Au, Pt, and NaCl.[7,8] However, such an EOS method of pressure calibration necessitates the use of x-ray diffraction techniques and is inconvenient for many experiments. Instead, it is often convenient to use the signal from a characteristic electronic transition as a secondary pressure calibration. Taking advantage of the optical accessibility of diamond anvil cells, several transitions in the visible light range were proposed for such a purpose, including ruby *R*1-*R*2, Sm:YAG (yttrium aluminum garnet),[9] etc. Among them, ruby fluorescence has been the most widely used.[1,7,8,10]

Ruby, $Al_2O_3:Cr_2O_3$ with typically 0.5 wt % Cr, has a corundum structure. The corundum structure does not experience a phase transition until above 80 GPa,[10] which makes it a convenient choice for pressure calibration over a wide pressure range. The optical transitions for the *R*1 and *R*2 fluorescence lines originate from a crystal field splitting of the local Cr^{3+} energy levels. Ruby fluorescence lines have been calibrated against the EOS of many cubic systems such as NaCl (Ref. 7) and noble metals[8] at room temperature. For other temperatures, it is widely assumed that the pressure induced frequency shift is temperature independent. However, this point has gone largely unchecked, especially at low temperatures where there exist only limited studies.[5,6] Nakano *et al.*[5] calibrated the ruby *R*1 line with the lattice constants of NaCl at T=10 K to P=22 GPa using nitrogen as the pressure medium. However, the theoretical calculation[11] that was used for the NaCl EOS assumed a temperature independent bulk modulus, which was unconfirmed and is likely incorrect. The other extant report[6] only measured the response to P=0.95 GPa, and the authors acknowledged that their pressure gauge at room temperature gave no direct measurements of the pressure in the frozen helium medium at T=4.2 K.

We first present a systematic study of the pressure inhomogeneity and anisotropy in both helium and methanol:ethanol 4:1 pressure media at T=5 K. Our work parallels a recent study by Klotz *et al.*[4] for 11 different pressure media at room temperature. We find equal levels of pressure inhomogeneity for helium and methanol:ethanol over the range $0<P<20$ GPa, with an approximately constant $\Delta P/P$ per unit area of $\pm 1.8\,\%/(10^4\ \mu m^2)$ throughout. The two pressure media also have comparable pressure anisotropy below 10 GPa, but start to differ at higher P.

We then present results of x-ray diffraction from weak charge density waves (CDWs) in single crystal samples of chromium at low temperature. While a less direct probe of the pressure conditions than our systematic study, this single crystal diffraction experiment is a more stringent test of pressure media for the application of greatest interest to condensed matter physics, namely, the accurate and precise measurement of vanishing order parameters in single crystal samples. We note that the sample-to-pressure chamber volume ratio plays a crucial role in providing a near-hydrostatic environment. For this reason, a methanol:ethanol 4:1 mixture is a better choice than helium for single crystal work below 10 GPa, while the helium pressure medium remains the ideal choice for powder or polycrystalline samples at all pressures.

Finally, we present an EOS-type calibration of the ruby *R*1 fluorescence line at T=4.5 K using silver as the pressure standard. The elastic properties of silver, a simple cubic metal, have been thoroughly studied at ambient pressure.[12–14] The isothermal bulk modulus of silver in the zero temperature limit was determined with high consistency to be $B_0=108.84\pm0.12$ GPa (Refs. 12–14) and, therefore, can be used for an accurate low temperature calibration of the ruby scale in the range $0<P<20$ GPa.

II. CHARACTERIZATION OF PRESSURE MEDIA AT T=5 K

The same preparation procedure for both the diamond anvil cell and the gasket was followed for all experiments presented in this paper. We used a home-built three-pin diamond anvil cell, and pressure was continuously adjusted using a helium gas membrane system. A pair of 800 μm culet diamond anvils was used together with 301-type stainless steel gaskets preindented to a thickness of 100–110 μm. The 420 μm diameter sample chamber was drilled by electrical discharge machining. Upon sealing, the cell was cooled to the base temperature of 5 K. The membrane system can tune the pressure continuously to within 0.05 GPa resolution at T=5 K without warming up, and this procedure was followed for all experiments presented here.

The use of a membrane allows one to change pressure *in situ* in a cryogenic environment, which is a departure from the typical procedure used in high-pressure research. For a condensed matter experiment at high-pressure one is often concerned with phenomena such as the scaling of physical properties in the close vicinity of a phase transition. Thus, it is important to precisely tune P in the cell at a given T so that the sample is accurately and correctly positioned in phase space. Without a membrane control system, or other mechanical lever-arm type of *in situ* tuning, one typically has to change pressure at room T, followed by either warming or cooling the cell to the desired temperature. From our own experience and other well-documented accounts in the literature, all pressure cells experience pressure variations due to thermal expansion or contraction of different cell body parts. This makes it impossible to precisely anticipate the pressure change upon cooling from room T to cryogenic temperatures, and prohibitively difficult to exercise fine control of pressure across a phase boundary. Furthermore, even pressure media that are liquid at room temperature typically freeze well before a pressure cell stops contracting upon cooling. This is indeed how pressure anisotropy and inhomogeneity develop. Therefore, the pressure disturbance on a sample may in fact be minimized by using a membrane to change the pressure *in situ*.

The degree to which a pressure medium deviates from hydrostatic can be characterized by inhomogeneity and anisotropy. The former measures the gradient in the stress tensor as one moves about the pressure chamber, while the latter measures the deviation of the stress tensor from isotropic. In order to characterize the pressure inhomogeneity and anisotropy, we used annealed synthetic ruby balls,[15] whose well-controlled shape and small size (20–30 μm diameter) allow

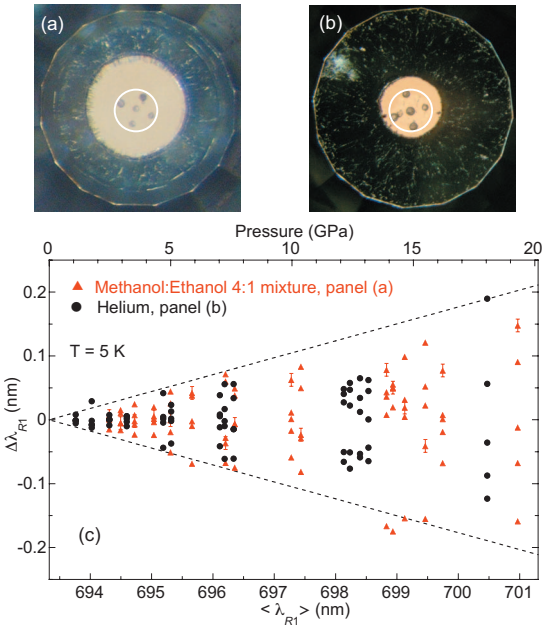

FIG. 1. (Color) Estimating the pressure inhomogeneity with spatially resolved ruby fluorescence measurements. [(a) and (b)] Micrographs of the sample pressure chamber, (a) loaded with a methanol:ethanol 4:1 mixture, compressed to 19.3 GPa at T=5 K, and warmed back to room temperature, (b) after an initial loading to 2 GPa with helium pressure medium at room temperature. The difference in sample chamber size is entirely due to the high compressibility of helium; both gaskets were initially prepared with same diameter holes and thickness. The five ruby balls in each sample chamber were used for both pressure inhomogeneity and anisotropy studies. The white circles delineate an area of interest 180 μm in diameter. (c) Variation in the five ruby $R1$ peak positions around the mean $\langle\lambda_{R1}\rangle$ for both pressure media up to 20 GPa. Error bars represent the uncertainty of individual peak positions and are only plotted for one ruby ball for the sake of clarity. The dashed lines model the range of this variation, which increases linearly with pressure and can be parameterized by a single inhomogeneity-per-unit-area ratio $\Delta P/P = \pm 1.8\%/(10^4\ \mu\text{m}^2)$. The pressure scale on the top x-axis represents our updated calibration described in Sec. IV.

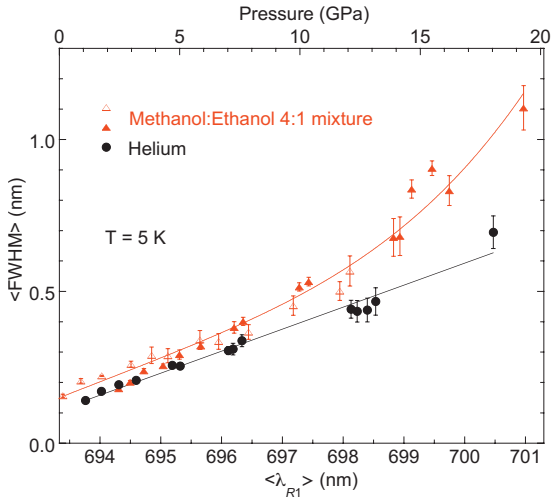

FIG. 2. (Color) FWHM of the ruby $R1$ fluorescence peaks at T=5 K for both pressure media up to P=20 GPa. Plotted values are the average for the five measured rubies at each pressure, error bars are the 1σ deviation for the estimator, and the abscissa $\langle\lambda_{R1}\rangle$ is the mean peak position for the five rubies. Full triangles are data from the experiments pictured in Figs. 1(a) and 1(b); empty triangles show data from a second experiment with the methanol:ethanol pressure medium, which was set up in almost the same manner as that pictured in Fig. 1(a) except that the placed five ruby balls covered a larger spatial area in the pressure chamber. The pressure scale on the top x-axis represents our updated calibration described in Sec. IV.

them to approximate point detectors of the stress tensor. Combined with an iris on the first image plane of our ruby spectroscopy setup, we were able to achieve position sensitivity by discriminating the fluorescence signal from individual ruby balls. For both pressure media, five ruby balls were placed in a cross pattern (covering approximately equal areas for the two pressure media) within the pressure chamber [Figs. 1(a) and 1(b)]. The helium pressure medium was loaded in the supercritical form at 20 000 psi (0.14 GPa) at room temperature, and both the helium- and alcohol-loaded cells were pressurized to 2 GPa before cooling from room temperature to 5 K. The final gasket thickness at the highest measured pressure was 41 μm at 18.0 GPa for helium and 62 μm at 19.3 GPa for methanol:ethanol. The opposing diamonds therefore never directly squeezed any ruby ball. A 532 nm diode laser (50 mW) was used for ruby fluorescence excitation. The effect of laser heating is negligible because the pressure cell was immersed in cold gas in a helium flow cryostat. This is confirmed by the ruby spectra, in which the thermally excited $R2$ peak was never observed. An Ocean Optics HR4000 spectrometer was used to collect the ruby spectrum. The spectrometer resolution was 0.05 nm full width at half maximum (FWHM), as calibrated by a mercury:argon source (Ocean Optics, HG-1).

We plot in Fig. 1(c) the deviation of the five ruby $R1$ fluorescence peak positions from their average value as a function of pressure for both the helium and methanol:ethanol pressure media. The apparent uniformity of the distribution of $R1$ peak positions (rather than Gaussian or bimodal) suggests that the pressure inhomogeneity $\Delta P/P$ is linearly dependent on the area of interest. There exist published accounts of pressure distributions in the sample chamber with a radial gradient.[1,16,17] We did not observe such a distribution possibly because our pressure inhomogeneity is much smaller than the gradients reported in the literature.[1,16,17] Instead of varying radially, the $R1$ peak position for each ruby ball varies randomly around the average value upon pressurizing [Fig. 1(c)]. The pressure inhomogeneity within a fixed area [Figs. 1(a) and 1(b)] is comparable for the helium and alcohol pressure media, and can be characterized by a single inhomogeneity-per-unit-area ratio $\Delta P/P = \pm 1.8\%/(10^4\ \mu\text{m}^2)$ as determined by the dashed lines in Fig. 1(c).

For an estimate of the pressure anisotropy at T=5 K, we plot in Fig. 2 the average FWHM of all five ruby $R1$ fluorescence peaks as a function of pressure. We note that even at ambient pressure the average peak width ($\sim 0.15 \pm 0.02$ nm) of the spherical rubies is not limited by the instrument resolution, and is four times larger than the sharpest $R1$ peak FWHM value (0.8 cm^{-1} or 0.038 nm) found in the literature.[2,18] Given the monotonic increase in $R1$ peak width with increasing Cr doping at room temperature, our ruby balls likely have a high Cr dopant concentration.[15] Nonetheless, the $R1$ peak FWHM at low temperature is significantly narrower than the corresponding width at room T (~ 0.55 nm), and remains a sensitive gauge of pressure anisotropy. Furthermore, since the variation of

$R1$ peak position around the average value is random for individual ruby balls [Fig. 1(c)], any systematic difference in Cr doping level is not affecting the present study.

For pressures below 10 GPa, there is no significant difference in the $R1$ FWHM for helium and methanol:ethanol pressure media. This is consistent with previous studies up to P=3 GPa at T=4.2 K.[2] For P>10 GPa, a significant difference develops and in this regime, helium may indeed provide an improved pressure environment. Spectroscopic measurements with ruby single crystals have shown orientation dependence upon uniaxial compression.[19] However, our rubies are polycrystalline and are thus insensitive to this effect. In the diamond anvil cell geometry, the maximum pressure anisotropy is bounded by the yield strength of the pressure medium.[20–23] In Secs. III and IV we attempt to estimate this value for both the methanol:ethanol and helium media using x-ray diffraction results at T=5 K.

III. EXPERIMENTAL CHOICE OF PRESSURE MEDIA

The measurements of pressure inhomogeneity and anisotropy described above are characteristic of a static pressure environment, with gradients that are not likely to relax during the time span of a single measurement. By contrast, a typical high-pressure experiment is comprised of a series of compressions of the sample chamber volume, each of which causes a rearrangement of the pressure environment with dynamic gradients that may be significant on the length scale of a typical sample and the time scale of a typical measurement. These time and length scales must be taken into consideration when designing a high-pressure experiment. In our experience, we found that a dynamic pressure environment at low temperature can damage a single crystal sample significantly more than might be expected from the inhomogeneity and anisotropy measured above.

Such problems arise when either the pressure chamber volume shrinks significantly or the sample occupies a significant fraction of the pressure chamber volume, and this speaks to the point of why one might choose alcohol over helium as the pressure medium for a given experiment. Helium has a high compressibility, and at P=20 GPa and T=5 K it typically sustains a sample volume that is only 1/8th of the bore size at an initial loading pressure of 0.14 GPa at room temperature; even at 2 GPa and room T, the sample volume has already shrunk by greater than a factor of 3 [Fig. 1(b)]. By comparison, with a methanol:ethanol mixture the chamber volume reduces by a factor of approximately 2 between a starting point at ambient pressure and room temperature, and an ending point at 20 GPa and 5 K [Fig. 1(a)]. To sustain a nearly hydrostatic sample environment it is believed necessary to keep a chamber-to-sample volume ratio of at least 10.[24] Furthermore, even for the same pressure medium, different cell assemblies can result in very different sample environments. For example, when testing the methanol:ethanol mixture pressure medium, Klotz *et al.*[4] used a 400 μm diamond culet, 150–200 μm initial gasket hole, and 40 μm preindentation thickness, resulting in a sample chamber volume which was about 1/10th of ours. Their ruby ball placement was similar to ours and over an area not larger than that shown in Fig. 1(a). However, they observed a pressure inhomogeneity with a 4.7 GPa FWHM (1σ=2 GPa) at 20 GPa and room T, in stark contrast to the full width of 1 GPa that we observe at 20 GPa and 5 K [Fig. 1(c)]. This discrepancy highlights our point that the choice of pressure medium is not the only deciding factor in designing an appropriate pressure environment, and that optimizing the cell assembly for the desired pressure range is equally important. Given the highly constrained geometry of a diamond anvil cell and the multiple, often-conflicting requirements on sample form factor, we found that a methanol:ethanol pressure medium provides a better pressure environment than helium for single crystal measurements at pressures up to 10 GPa and at all cryogenic temperatures.

In evaluating the effect of a dynamically evolving, nonhydrostatic pressure medium on our samples we find that the crystal mosaic is the most relevant discriminator. Unlike local spectroscopic probes, such as ruby fluorescence and nuclear quadrupole resonance,[25] the crystal mosaic of a given sample records the history of damage over the course of an experiment, and the measured rocking curves integrate over the sample volume. To illustrate this method of assessment, we provide here a successful example of maintaining high-quality, single crystal metallic samples in a methanol:ethanol 4:1 medium at high pressure and low temperature.

Presented in Fig. 3 is a brief overview of the experimental setup and raw data from recent x-ray diffraction work on the CDW and spin density wave in the elemental antiferromagnet chromium under pressure.[26–28] Chromium possesses a body-centered cubic structure with spin and CDWs that are characterized by an incommensurate modulation vector $\boldsymbol{Q}$. The cubic symmetry leads to a threefold degenerate domain structure, and it is well known that $\boldsymbol{Q}$ points with equal probability along any of the three cubic axes in an unbiased crystal, resulting in an equal volumetric distribution of spatially distinct Q-domains. The degeneracy between the three domain configurations is easily lifted by a uniaxial stress[29,30] or even residual surface stress from sample preparation.[31] It is well documented[29,30] that at ambient conditions, a uniaxial stress at the level of 0.7–0.9 kg/mm^2 (equivalently 0.007–0.009 GPa) will induce a single Q-domain state. For our high-pressure experiment on chromium, it is therefore important to observe the sample in a multiple Q-domain configuration[26,27] to rule out a uniaxially compressed sample condition. This represents a stringent, although indirect, test of the sample environment in a diamond anvil cell.

Our pressure chamber assembly [Fig. 3(a)] includes a single crystal chromium sample of size $55\times70\times30$ μm^3 on which weak CDW superlattice diffraction peaks were measured at pressures up to 9.5 GPa.[28] In Figs. 3(c)–3(j) we present raw diffraction scans of the CDW and lattice peaks at T=5.8 K and P=8.9 GPa (for data at 9.5 GPa, see Ref. 28). This same sample was pressurized from 3.2 to 9.9 GPa *in situ* in a methanol:ethanol pressure medium at T=5.8 K, and the sample mosaic FWHM was maintained at or below 0.08° throughout [Figs. 3(c) and 4]. The very fact that all three cubic CDW domains were observed [Figs. 3(e)–3(j)] is indicative of a highly isotropic pressure environment, and the

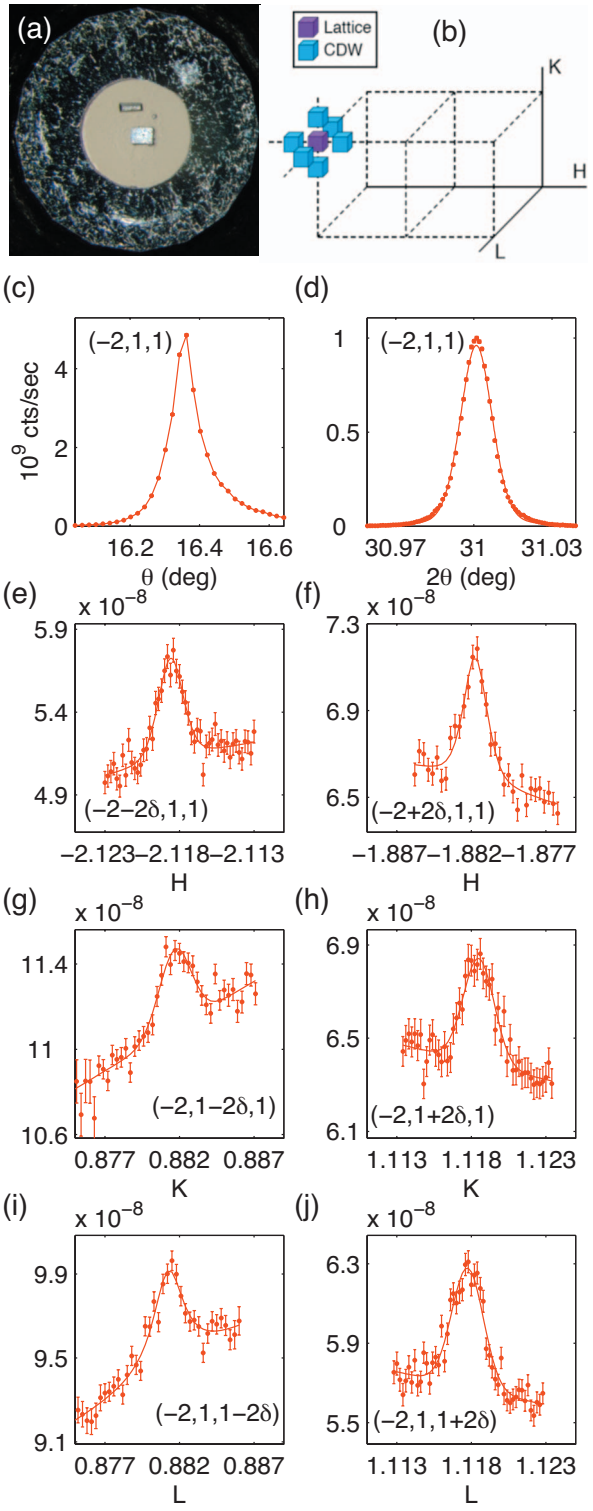

FIG. 3. (Color) Experimental setup and raw data from recent x-ray diffraction measurements of the CDW in chromium under pressure (Refs. 26–28). All data shown here were measured at T=5.8 K and P=8.9 GPa. (a) Micrograph of the sample chamber showing the oriented single crystal sample, as well as Ag foil and a ruby ball used as manometers. The diamond culet, 800 μm in diameter, spans the field of view. (b) Schematic of diffraction geometry showing central (211)-type lattice Bragg peak surrounded by six CDW satellite peaks, each of which is removed from the central peak by a distance 2δ. [(c) and (d)] Rocking curve and radial θ-2θ scans through a (211)-type lattice Bragg peak. [(e)–(j)] *hkl* scans through the six surrounding CDW peaks. Count rates are normalized to that of the lattice peak. The x-ray energy was 20.000 keV.

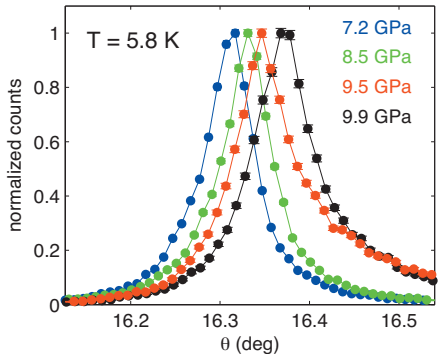

FIG. 4. (Color) Rocking curves of a (211)-type lattice Bragg peak recorded during an x-ray diffraction measurement of the CDW in chromium under pressure (Refs. 26–28). Sample micrograph appears in Fig. 3(a); the peak shown in Fig. 3(c) also belongs to this series. The pressure was increased from 3.2 to 9.9 GPa *in situ* at T=5.8 K in a methanol:ethanol pressure medium.

deviatoric stress is estimated to be less than 0.01 GPa at 9 GPa.[27] The correlation between improved sample mosaicity and increasing chamber-to-sample volume ratio is evident through a series of published micrographs in the literature [Fig. 1(b) of Ref. 26, Fig. 1(c) of Ref. 27, and Fig. 3(a)]. Given the pressure inhomogeneity measured above and the size of the Cr sample under consideration, we estimate $\Delta P/P = \pm 0.69\%$ or $\Delta P = \pm 0.062$ GPa across the sample surface, consistent with our previous estimation based on the observed pressure broadening of radial θ-2θ diffraction scans of the lattice Bragg peaks.[27]

We have demonstrated the quality of a methanol:ethanol 4:1 mixture as a pressure medium for cryogenic single crystal experiments at pressures up to 10 GPa. The ratio of pressure chamber-to-sample volume, which is related to the compressibility of the pressure medium, is a key parameter in providing near-hydrostatic conditions and may be more important in this regard than the choice of pressure medium. On the other hand, given the measured pressure anisotropy above 10 GPa, helium remains the ideal pressure medium for experimental work on powders and polycrystals over a wide range of pressure and temperature (cf. Ref. 32, where helium was used to pressurize single crystal samples at room temperature up to P=39 GPa). It remains unclear how to preserve single crystal samples at low temperature for pressures much beyond 10 GPa, and further experimental work is necessary to clarify this issue. The above considerations suggest that, due to their relatively low compressibility, nitrogen, neon, or argon might serve well as pressure media for single crystals at cryogenic temperature for P > 10 GPa.[2,4]

IV. RUBY PRESSURE SCALE CALIBRATION AT T=4.5 K

For calibrating the ruby $R1$ fluorescence secondary pressure scale at low temperature, we chose a well-characterized synthetic ruby specimen from Alfa Aesar (No. 36206). The bulk specimen (1.6 mm in diameter) was optically transparent and spatially uniform in color. Using an ion microprobe we determined the Cr concentration to be 0.47 ± 0.01 wt %. This is consistent with the prevalent choice of ruby in the literature.[5,7,15,18,19] Polycrystalline silver foil (Alfa Aesar, No.

42472, 99.998%) of 25 μm thickness and annealed temper was placed in the pressure chamber together with a shard of ruby, and the cell was loaded with condensed helium gas as described above.

The diamond anvil cell was mounted on the cold finger of a Gifford–MacMahon-type cryostat (Sumitomo 205E), which was in turn mounted on a precision x-y-z translation stage on the sample stage of an x-ray diffractometer. The measurement temperature was 4.5 ± 0.5 K. An unpressurized cell was cooled first and both silver diffraction and ruby $R1$ fluorescence were measured to establish the ambient pressure point. The pressurized diamond anvil cell was subsequently cooled, and the helium-controlled membrane was used to increase pressure *in situ*. An Ocean Optics HR4000 spectrometer (different from that used in Sec. II) was used to collect the spectrum, with a wide instrument resolution of 0.22 nm FWHM measured with a mercury:argon source (Ocean Optics, HG-1).

Data were collected using two different high-resolution x-ray diffractometers, at beamlines 4-ID-D and 11-ID-C at the Advanced Photon Source. At 4-ID-D, a Huber psi-circle diffractometer was used in the vertical scattering geometry, with a NaI point detector on the 2θ arm. This instrument eliminates uncertainties related to both the zero position and the overall scale of 2θ, which are issues commonly encountered with image-plate powder diffraction techniques. The extremely small vertical angular divergence of an insertion device x-ray beam combined with 50 μm wide vertical detector slits at a distance 1.3 m along the 2θ arm from the sample allows a high q resolution, $\Delta q(\mathrm{FWHM}) \sim 1 \times 10^{-3}$ Å^{-1}. The 20.000 keV x-ray beam was calibrated with the Mo K-edge, monochromatized by a double-bounce Si (111) monochrometer, and focused by a pair of palladium mirrors.

At 11-ID-C,[33] the unfocused high-energy x-ray beam (114.97 keV) from the undulator was monochromatized by a Si (311) single crystal. The x-ray energy was calibrated by comparing the energy spectrum with ^{57}Co and ^{109}Cd sources. A Si (220) crystal analyzer was placed on the analyzer stage, 1194 mm away from the sample. The instrument resolution was $\Delta q(\mathrm{FWHM}) \sim 3 \times 10^{-3}$ Å^{-1}. The instrument resolutions of our x-ray diffraction setups and ruby fluorescence detection are well matched as can be seen in Fig. 5, where we compare line shapes of both the ruby $R1$ fluorescence and the silver (111) diffraction peaks measured at 4-ID-D, for pressures between 0 and 15.8 GPa. The high-resolution x-ray powder diffraction is indeed as sensitive as ruby fluorescence in measuring the pressure.

For the pressure calibration, the first five orders of silver diffraction [(111), (200), (220), (311), and (222)] were measured together with the ruby $R1$ fluorescence at each pressure. In Fig. 6 we present the measured silver lattice constant versus the peak position of ruby $R1$ fluorescence at T=4.5 K.

In order to convert from silver lattice constant to pressure, we used the one-parameter Birch equation $P=(3/2)B_0[(a_0/a)^7-(a_0/a)^5]$ (the $B'=4$ special case of the BE1 equation in Ref. 34), where $a_0=4.0683 \pm 0.0002$ Å is our measured silver lattice constant at T=4.5 K. A linear

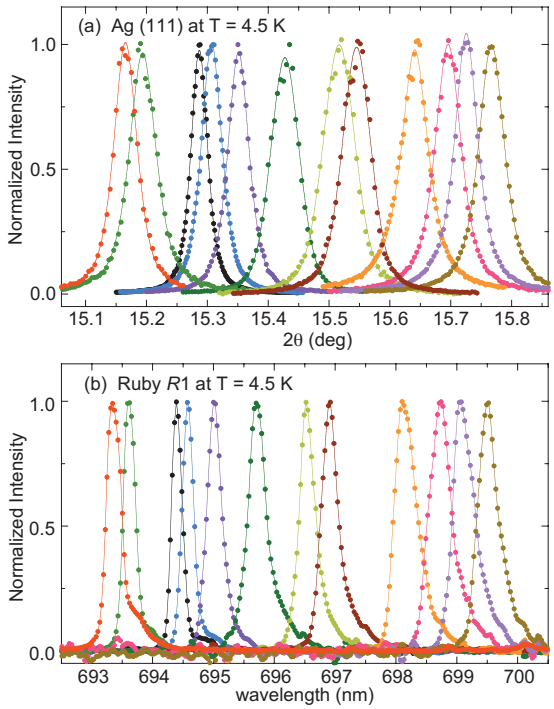

FIG. 5. (Color) Comparison of line shapes of x-ray powder diffraction and ruby fluorescence under pressure. (a) High resolution x-ray (111) powder diffraction peaks from Ag, measured at Sector 4-ID-D of the Advanced Photon Source at T=4.5 K for pressures 0 to 15.8 GPa. (b) Ruby $R1$ fluorescence lines corresponding to the pressure series shown in (a). The silver diffraction scans are not limited by the instrument resolution (0.0085° FWHM); the ruby fluorescence measurements are not limited by the instrument resolution (0.22 nm FWHM) above 4 GPa.

relationship between the ruby $R1$ wavelength and pressure is observed over the measured range from 0 to 15.8 GPa, with $P=A_0 \ln(\lambda/\lambda_0)$ and $A_0=1762 \pm 13$ GPa (Fig. 7). The ruby pressure coefficient A_0 was summarized in a recent review,[10] with a best estimate $A_0=1868 \pm 30$ GPa at room temperature. Our result at T=4.5 K is significantly different.

Possible systematic errors in our measurement could

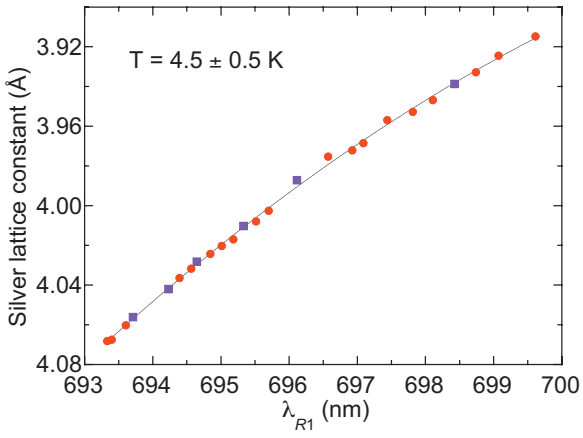

FIG. 6. (Color) Measured silver lattice constant vs peak of ruby $R1$ fluorescence. Solid red circles: data taken with the psi-circle diffractometer at 4-ID-D, using 50 μm vertical detector slits at a distance 1.3 m along the 2θ arm from the sample. Solid purple squares: data taken at 11-ID-C, using a Si(220) single crystal analyzer. The silver lattice constants were calculated by a σ^2-weighted average of five measured diffraction orders. Measurement uncertainties are smaller than the symbol size unless shown. The solid line is a guide to the eye.

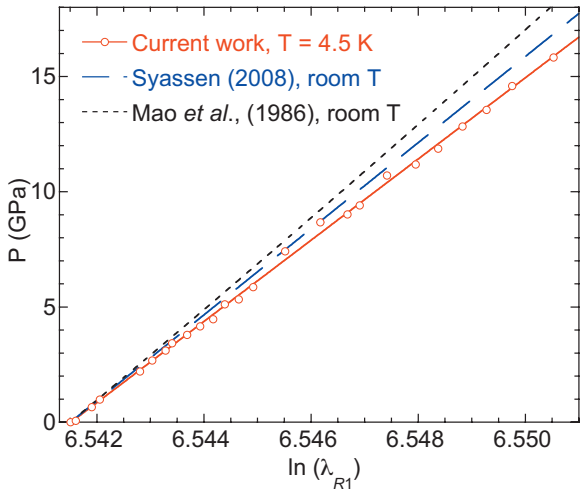

FIG. 7. (Color) Ruby pressure scale at T=4.5 K. Pressure was calculated using the silver bulk modulus 108.84 GPa and the one-parameter Birch EOS. The linear fit (solid red line) up to 15.8 GPa gives the calibration $A_0 = dP/d\ln(\lambda) = 1762 \pm 13$ GPa for the ruby $R1$ line at T=4.5 K. For comparison we also plot an updated calibration of ruby at room T [blue long dashed line; Eq. (26) of Ref. 10 with $A_0 = 1868$ GPa], as well as an early nonlinear calibration, $P = A_0/B[(\lambda/\lambda_0)^B - 1]$ with $A_0 = 1904$ GPa and $B = 7.665$ (black short dashed line, Ref. 8), which was established for a wide pressure range below 80 GPa at room T.

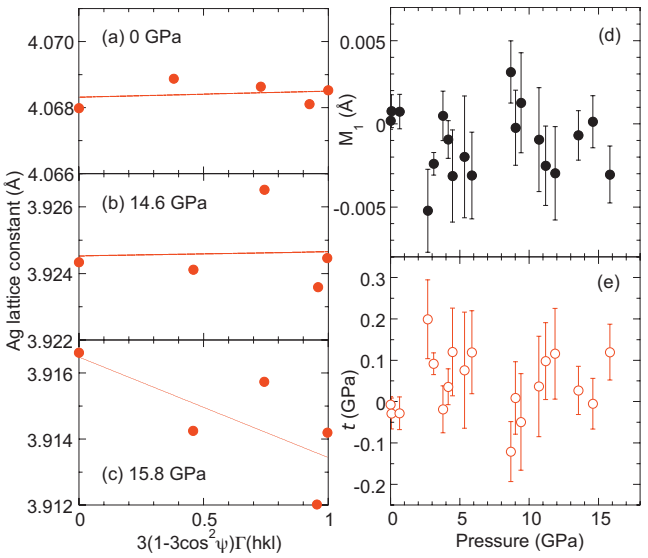

FIG. 8. (Color) Estimation of pressure anisotropy in a diamond anvil cell at T=4.5 K. [(a)–(c)] Lattice constant a_{hkl} measured at each diffraction order (hkl) is plotted against $[3(1-3\cos^2\psi)\Gamma(hkl)]$ for pressures at 0, 14.6, and 15.8 GPa, respectively. The last two are the highest pressure points in our Ag lattice measurement. (d) Plot of slope M_1 vs P. (e) Plot of deviatoric stress t as a function of pressure. Note that most measured values are less than a 1-σ variation from zero, and that there is no apparent pressure dependence. We estimate the pressure anisotropy to be 0.021 ± 0.011 GPa.

come from the effects of both pressure inhomogeneity and anisotropy (deviatoric stress) inside the sample chamber. For pressure media such as helium and the methanol:ethanol mixture, the deviatoric stress is typically one order of magnitude smaller than the pressure inhomogeneity. For example, in Sec. III and previously in Ref. 27, we estimated the pressure anisotropy in methanol:ethanol medium to be about 0.01 GPa at 9 GPa, while pressure inhomogeneity across the Cr sample is about 0.1 GPa.

The shear strength of solid helium was estimated to be 0.3–0.5 GPa at room T and P=150 GPa.[23] Using the data set taken at 4-ID-D we can estimate the deviatoric stress between 0 and 16 GPa at 5 K using a procedure that is well documented in the literature.[22,23] The lattice constant a_{hkl} measured at each (hkl) order is related to the deviatoric stress t through $a_{hkl} = M_0 + M_1[3(1-3\cos^2\psi)\Gamma(hkl)]$, where ψ is the angle between the transferred momentum and the anvil compression axis, $\Gamma(hkl) = (h^2k^2 + k^2l^2 + l^2h^2)/(h^2 + k^2 + l^2)^2$, $M_1 = -a_P(\alpha t S/3)$, and M_0 is essentially constant given that ψ in our measurements was always between 82° and 90°. Other parameters in the above expression are a_P, the lattice constant, a unitless constant α which is approximately unity for our nearly continuous stress sample environment, and $S = (1/C' - 1/C)/2$.[23] Using the elastic shear moduli C and C' for silver at ambient P and the T=0 limit,[12] we calculate $S = 0.0195$ GPa^{-1}.

In Figs. 8(a)–8(c), we plot the measured a_{hkl} versus $[3(1-3\cos^2\psi)\Gamma(hkl)]$ for all five orders of silver diffraction measured at 0, 14.6, and 15.8 GPa, respectively. The slope of the linear fit generates M_1, which is plotted against pressure in Fig. 8(d). Most M_1's are consistent with zero, within 1-σ uncertainty, indicating that the lattice measured at each order is nearly isotropically compressed. In Fig. 8(e), we plot the calculated deviatoric stress t using the numerical values given above. Since there is no apparent pressure dependence, we report the σ^2-weighted average value 0.021 ± 0.011 GPa as the best estimation of the deviatoric stress t up to 15.8 GPa. In our current setup, this value is smaller than the pressure inhomogeneity (Fig. 1).

Another systematic error in our calibration could come from the use of the one-parameter Birch equation for the silver EOS. Other nonlinear EOS such as the two-parameter Birch equation $P = (3/2)B_0[(a_0/a)^7 - (a_0/a)^5]\{1 + (3/4)(B' - 4)[(a_0/a)^2 - 1]\}$ [Eq. (BE1) in Ref. 34] or the Murnaghan equation $P = (3/2)B_0[(a_0/a)^{B'} - 1]$ involve the first pressure derivative of the bulk modulus $B' = dB/dP$. Unfortunately the value of B' is not well established for silver at low temperature and varies in the literature from 3.66 to 6.16 at room T.[35] Using a value of $B' = 4$ would leave our result unchanged, while a larger B' would curve the data in Fig. 7 upward. Our confidence in the one-parameter Birch equation thus comes from the linearity of the measured data in Fig. 7. The slope A_0 is unchanged if one fits over data only below 6 GPa, corresponding to a pressure range about 5% of the silver bulk modulus, for which the one-parameter Birch equation is expected to be highly accurate. Likewise, the ruby wavelength shift is expected to be linear with pressure over our measured range, as our highest pressure of 15.8 GPa is only 6.2% of the ruby bulk modulus of 253 GPa.[10] This is also consistent with the observed linear behavior up to P=20 GPa at room temperature.[7]

V. CONCLUSIONS

We characterized the pressure inhomogeneity and anisotropy at T=5 K over a range of pressures, $0 < P < 20$ GPa, for two representative pressure media, helium and a methanol:ethanol 4:1 mixture. Using the same preparation

conditions, both media show equivalent levels of inhomogeneity up to P=20 GPa and comparable anisotropy up to 10 GPa. For P>10 GPa, the helium medium provides a smaller anisotropy. The pressure inhomogeneity in the two media has a linear dependence on both area and pressure, and is characterized by a constant ratio $\Delta P/P$ per unit area of $\pm 1.8\,\%/(10^4\ \mu m^2)$.

These two pressure media were also considered for use in single crystal x-ray diffraction experiments, taking into account the operational details of pressure history and sample quality requirements. We found that the pressure-chamber-to-sample volume ratio is a key parameter in providing a high-quality pressure environment, and for this reason the methanol:ethanol mixture is preferred to helium for single crystal work at pressures under 10 GPa. The question of an appropriate pressure medium for single crystal experiments beyond 10 GPa at low temperatures requires further investigation.

We also performed a direct calibration of the pressure scale of the ruby $R1$ fluorescence line at T=4.5 K using the silver lattice constant and its known EOS. Using data between 0 and 15.8 GPa, we determined the linear coefficient $A=-dP/d(\ln \lambda)=1762\pm 13$ GPa for the ruby $R1$ line at T=4.5 K. This result shows that the ruby pressure scale is temperature dependent between cryogenic and room temperatures, and contrary to common practice leads to a necessary pressure correction of more than 0.5 GPa at 10 GPa. Our low temperature calibration should hold for all T<50 K, over which the bulk moduli of both Ag and ruby are constant. Further work remains for the calibration of the ruby scale for P>20 GPa, where the linear relationship is no longer expected to hold.

ACKNOWLEDGMENTS

We acknowledge discussions and technical help from V. Prakapenka and P. Dera, and the use of the helium loading facility at GeoSoilEnviroCARS (Sector 13), Advanced Photon Source, Argonne National Laboratory. We are also grateful to I. Steele for the ion microprobe characterization of the Alfa Aesar ruby specimen, and D. Heinz for discussion of the Birch equations. In addition, we thank the staff of Sector 4 at the Advanced Photon Source, specifically J. Lang and Z. Islam for their help with x-ray diffraction, and D. Haskel and N. Souza-Neto for their help with the ruby spectrometer. GSE-CARS was supported by the National Science Foundation-Earth Sciences (Grant No. EAR-0622171) and U.S. Department of Energy-Geosciences (Grant No. DE-FG02-94ER14466). The work at the University of Chicago was supported by the National Science Foundation-Division of Materials Research (Grant No. DMR-0907025). Use of the Advanced Photon Source was supported by the U.S. DOE-BES under Contract No. DE-AC02-06CH11357.

[1] G. J. Piermarini, S. Block, and J. D. Barnett, J. Appl. Phys. **44**, 5377 (1973).
[2] J. H. Burnett, H. M. Cheong, and W. Paul, Rev. Sci. Instrum. **61**, 3904 (1990).
[3] K. Takemura, J. Appl. Phys. **89**, 662 (2001).
[4] S. Klotz, J.-C. Chervin, P. Munsch, and G. Le Marchand, J. Phys. D: Appl. Phys. **42**, 075413 (2009).
[5] K. Nakano, Y. Akahama, Y. Ohishi, and H. Kawamura, Jpn. J. Appl. Phys., Part 1 **39**, 1249 (2000).
[6] B. A. Noack and W. B. Holzapfel, in *High Pressure Science and Technology*, edited by K. D. Timmerhaus and M. S. Barber (Plenum, New York, 1979), p. 748.
[7] G. J. Piermarini, S. Block, J. D. Barnett, and R. A. Forman, J. Appl. Phys. **46**, 2774 (1975).
[8] H. K. Mao, J. Xu, and P. M. Bell, J. Geophys. Res. **91**, 4673, doi:10.1029/JB091iB05p04673 (1986).
[9] N. J. Hess and D. Schiferl, J. Appl. Phys. **68**, 1953 (1990).
[10] K. Syassen, High Press. Res. **28**, 75 (2008).
[11] E. F. Skelton, A. W. Webb, S. B. Qadri, S. A. Wolf, R. C. Lacoe, J. L. Feldman, W. T. Elam, E. R. Carpenter, and C. Y. Huang, Rev. Sci. Instrum. **55**, 849 (1984).
[12] D. R. Smith and F. R. Frickett, J. Res. Natl. Inst. Stand. Technol. **100**, 119 (1995).
[13] J. R. Neighbours and G. A. Alers, Phys. Rev. **111**, 707 (1958).
[14] S. N. Biswas, P. Van't Klooster, and N. J. Trappeniers, Physica B & C **103**, 235 (1981).
[15] J. C. Chervin, B. Canny, and M. Mancinelli, High Press. Res. **21**, 305 (2001).
[16] R. Boehler, Rev. Geophys. **38**, 221, doi:10.1029/1998RG000053 (2000).
[17] C. Meade and R. Jeanloz, J. Geophys. Res. **93**, 3261, doi:10.1029/JB093iB04p03261 (1988).
[18] D. D. Ragan, R. Gustavsen, and D. Schiferl, J. Appl. Phys. **72**, 5539 (1992).
[19] X. A. Shen and Y. M. Gupta, Phys. Rev. B **48**, 2929 (1993).
[20] A. L. Ruoff, J. Appl. Phys. **46**, 1389 (1975).
[21] W. A. Bassett, J. Phys.: Condens. Matter **18**, S921 (2006).
[22] A. K. Singh and T. Kenichi, J. Appl. Phys. **90**, 3269 (2001).
[23] A. Dewaele and P. Loubeyre, High Press. Res. **27**, 419 (2007).
[24] V. Prakapenka, private communication (2009).
[25] H. Fukazawa, K. Hirayama, T. Yamazaki, Y. Kohori, and T. Matsumoto, J. Phys. Soc. Jpn. **76**, 125001 (2007).
[26] Y. Feng, R. Jaramillo, G. Srajer, J. C. Lang, Z. Islam, M. S. Somayazulu, O. G. Shpyrko, J. J. Pluth, H.-k. Mao, E. D. Isaacs, G. Aeppli, and T. F. Rosenbaum, Phys. Rev. Lett. **99**, 137201 (2007).
[27] R. Jaramillo, Y. Feng, J. C. Lang, Z. Islam, G. Srajer, H. M. Rønnow, P. B. Littlewood, and T. F. Rosenbaum, Phys. Rev. B **77**, 184418 (2008).
[28] R. Jaramillo, Y. Feng, J. C. Lang, Z. Islam, G. Srajer, P. B. Littlewood, D. B. McWhan, and T. F. Rosenbaum, Nature (London) **459**, 405 (2009).
[29] T. J. Bastow and R. Street, Phys. Rev. **141**, 510 (1966).
[30] T. Matsumoto and T. Mitui, J. Phys. Soc. Jpn. **25**, 634 (1968).
[31] J. P. Hill, G. Helgensen, and D. Gibbs, Phys. Rev. B **51**, 10336 (1995).
[32] D. L. Farber, D. Antonangeli, C. M. Aracne, and J. Benterou, High Press. Res. **26**, 1 (2006).
[33] U. Rütt, M. A. Beno, J. Strempfer, G. Jennings, C. Kurtz, and P. A. Montano, Nucl. Instrum. Methods Phys. Res. A **467–468**, 1026 (2001).
[34] F. Birch, J. Geophys. Res. **83**, 1257, doi:10.1029/JB083iB03p01257 (1978).
[35] K. Syassen and W. B. Holzapfel, J. Appl. Phys. **49**, 4427 (1978).